Journal of Zhejiang University-SCIENCE A (Applied Physics & Engineering)
ISSN 1673-565X (Print); ISSN 1862-1775 (Online)
www.zju.edu.cn/jzus; www.springerlink.com
E-mail: kwhlee@berkeley.edu

A novel non-iterative shape method for estimating the decay time constant of the finger photoplethysmographic pulse*

Ling-xiao HOU[†1], Ming WEI[3], Xuan WANG[1], Xin-zhong CHEN[2], Ying FENG[2], Kai JIANG[†‡1]

([1]*Key Laboratory of Biomedical Engineering of Ministry of Education, Department of Biomedical Engineering, Zhejiang University, Hangzhou 310027, China*)

([2]*Department of Anaesthesia, Women's Hospital, Hangzhou 310006, China*)

([3]*Institute of Space Medical Engineering, Beijing 100094, China*)

[†]E-mail: beasthlx@163.com; jiangkai1979@vip.sina.com

Received Aug. 27, 2010; Revision accepted Feb. 21, 2011; Crosschecked May 24, 2011

Abstract: The photoplethysmogram (PPG) of a pulse wave, similar in appearance to the arterial blood pressure (ABP) waveform, contains rich information about the cardiovascular system. The decay time constant RC, equal to the product of peripheral resistance *R* and total arterial compliance *C*, is a meaningful cardiovascular model parameter in vascular assessment. Using or ameliorating the existing ABP methods does not achieve a satisfactory estimation of RC from the PPG volume pulse (VRC). Thus, a novel non-iterative shape method (NSM) of evaluating VRC is introduced in this paper. The mathematic expression between a novel, readily available morphological parameter called the area difference ratio (ADR) and VRC was established. As it was difficult to calculate VRC from the complicated expression analytically, we recommend estimating it using a piecewise linear interpolation criterion. Also, since the effect of the PPG magnitude is eliminated in the calculation of ADR, precaliberation or normalization is dispensable in the NSM. Results of human experiments indicated that the NSM was computationally efficient, and the simulation experiments confirmed that the NSM was theoretically available for ABP.

Key words: Photoplethysmogram (PPG), Decay time constant, Non-iterative shape method (NSM), Area difference ratio (ADR)
doi:10.1631/jzus.A1000386 **Document code:** A **CLC number:** R318

1 Introduction

The photoplethysmogram (PPG) of a pulse wave is a non-invasive, readily available optical signal concerned with blood volume pulsations in the microvascular bed of tissue (Allen, 2007). Many features of unclear physiological significance have been investigated, including beat-to-beat PPG amplitude, area, and notch amplitude (Seitsonen *et al.*, 2005; Ahonen *et al.*, 2007; Huiku *et al.*, 2007). However, baseline drift induced by environmental conditions, metabolic state, human motion, and even mental state complicates the extraction and interpretation of those parameters (Zahedi *et al.*, 2007; Reisner *et al.*, 2008). As it is difficult to remove baseline wander without altering the wave shape and the PPG pulse is similar in morphology to arterial blood pressure (ABP) pulse, contemporary studies have concentrated on using or ameliorating the existing ABP shape methods to determine cardiovascular parameters from the PPG (Haffty *et al.*, 1983; Shimazu *et al.*, 1986; Yamakoshi and Kamiya, 1987; Seki, 1988; Lopez-Beltran *et al.*, 1998; Millasseau *et al.*, 2000; Miyai *et al.*, 2001; Hashimoto *et al.*, 2002; Millasseau *et al.*, 2003; Marcinkevics *et al.*, 2009).

The decay time constant RC, which is equal to the product of peripheral resistance *R* and total arterial compliance *C* and associated with the pathophysiologic changes of the cardiovascular system

‡ Corresponding author

* Project (No. 81070885) supported by the National Natural Science Foundation of China

(Fogliardi *et al.*, 1996; Eyal *et al.*, 1997; Gnudi, 1998; Segers *et al.*, 1999), is helpful in vascular assessment. The previous ABP non-shape methods for estimating RC (Yin and Liu, 1989; Shim *et al.*, 1994; Segers *et al.*, 1999; Stergiopulos *et al.*, 1999; Westerhof *et al.*, 2009), are not suitable for PPG, as those methods require pulsatile pressure data alone or in combination with flow data. A shape approach, based on fitting the measured pulse to a function of exponential type by applying a non-linear least squares criterion (Randall *et al.*, 1984; Eyal *et al.*, 1997; Wang *et al.*, 2003), appears feasible to calculate RC from the PPG volume pulse (VRC). Nevertheless, the concomitant problem of convergence makes the iterative non-linear least squares fitting method (LSM) non-optimal (Gnudi, 1998).

Thus, this paper deals with a novel non-iterative shape method (NSM) to estimate VRC, which is computationally efficient, and is not only suitable for PC, but also competent for embedded systems. Another contribution is to introduce a novel morphological parameter called the area difference ratio (ADR), and to establish a mathematic expression between ADR and VRC. Since ADR is independent of the PPG magnitude, precalibration or normalization is dispensable in the NSM.

2 Materials and methods

2.1 Data acquisition

Finger PPG signals were recorded in four healthy volunteers aged (25±2) yr and 17 anaesthetized patients aged (37±11) yr over 10 min after hemodynamic conditions were stable. The study was approved by the local Research Ethics Committee, and written informed consent was obtained from all participants.

2.2 Mathematic expression between the area difference ratio (ADR) and the decay time constant of the PPG volume pulse (VRC)

ADR was derived from the diastolic contour of the pulse. Fig. 1 shows a representative beat of the PPG pulse. *P* and *U* represent onset and end of diastole at time T_p and T_p+T_d, and T_d is the diastolic duration. $Y(t)$ is the time course of measured PPG pulse during diastole, and $P(t)=a+be^{-t/\mathrm{VRC}}$ ($T_p<t<T_p+T_d$, and *a* and *b* account for the initial conditions), is the corresponding two-element Windkessel model prediction. Fig. 2 is a further magnification of diastole shown in Fig. 1. *B* represents the intersection of the horizontal line and vertical line to the time axis. P_p and P_{pd} denote the measured magnitudes of *P* and *U*, respectively.

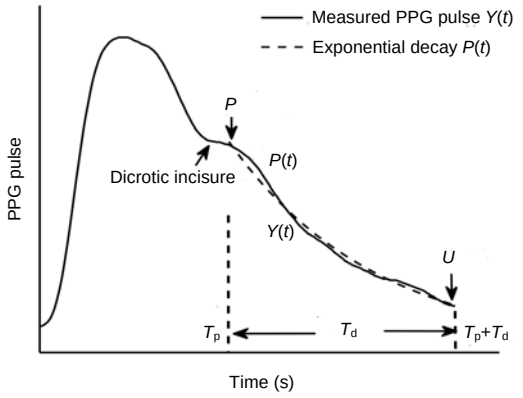

Fig. 1 A representative beat of photoplethysmogram (PPG) pulse

T_d: diastolic duration; *P* and *U*: onset and endpoint of diastole at time T_p and T_p+T_d, respectively

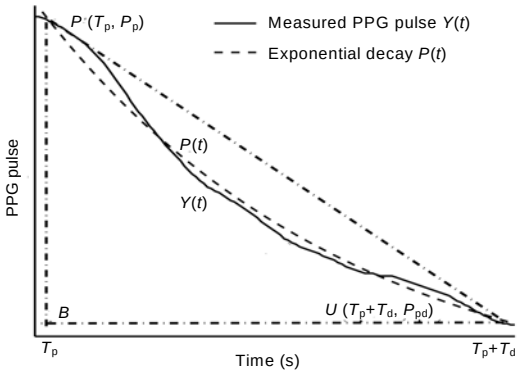

Fig. 2 A further magnification of diastole shown in Fig. 1

B: intersection of the horizontal line and vertical line to the time axis; P_p and P_{pd}: measured magnitudes of onset and end of diastole, respectively

ADR of a single beat, as illustrated in Figs. 1 and 2, could be calculated as the difference between the area of triangle ΔPUB (S_t) and the area under the curve of pulse $Y(t)$, but above the horizontal line *BU* (S_p) divided by S_t:

$$\mathrm{ADR}=\frac{S_t-S_p}{S_t}, \tag{1}$$

where $S_t=(P_p-P_{pd})T_d/2$, and S_p could be calculated by definite integral: $S_p=\int_{T_p}^{T_p+T_d}(Y(t)-P_{pd})\mathrm{d}t$.

Thus, for each isolated heart beat, ADR was readily available. Assuming the measured pulse $Y(t)$ decayed as the model prediction $P(t)$, we found ADR was only dependent on VRC and T_d if $Y(t)$ was substituted by $P(t)$:

$$\mathrm{ADR}=1+\frac{2\mathrm{e}^{-T_d/\mathrm{VRC}}}{1-\mathrm{e}^{-T_d/\mathrm{VRC}}}-\frac{2\mathrm{VRC}}{T_d}. \tag{2}$$

2.3 Piecewise linear interpolation

Suppose ADR, T_d, and VRC of the observed beat satisfied the expression:

$$\mathrm{ADR}_o=1+\frac{2\mathrm{e}^{-T_{do}/\mathrm{VRC}_o}}{1-\mathrm{e}^{-T_{do}/\mathrm{VRC}_o}}-\frac{2\mathrm{VRC}_o}{T_{do}}. \tag{3}$$

Note that the intricacy of Eq. (3) precluded the precise computation of VRC_o. Thus, we suggested estimating VRC_o using a piecewise linear interpolation criterion. Details are described in the following. Substituting T_{do} into Eq. (2), we could obtain a discrete set of data points (VRC(i), ADR(i)), while VRC(i) was progressively increased in steps varying from 0.01 to 20 based on clinical experience (Fogliardi *et al.*, 1996; Segers *et al.*, 1999). To assure the optimal step size of VRC, we tried different step size values and evaluated the relative error of estimation (RE_e), which is defined as

$$\mathrm{RE}_e=\frac{\mathrm{LIE}}{\mathrm{VRC}}\times 100\%, \tag{4}$$

where LIE represents the linear interpolation error, which is proportional to the second derivative and the square of step size. Concerned about the balance between the computational complexity and accuracy requirement, the optimal step size was determined to be 0.01. Fig. 3 exemplifies the curves of RE_e intuitively as the relative errors are less than 3% when step size is set to be 0.01.

Thereafter, piecewise linear interpolation was performed in the direction of ADR as follows:

$$\begin{aligned}\mathrm{VRC}_o=&\frac{\mathrm{ADR}_o-\mathrm{ADR}(k+1)}{\mathrm{ADR}(k)-\mathrm{ADR}(k+1)}\mathrm{VRC}(k)\\&+\frac{\mathrm{ADR}_o-\mathrm{ADR}(k)}{\mathrm{ADR}(k+1)-\mathrm{ADR}(k)}\mathrm{VRC}(k+1),\end{aligned} \tag{5}$$

where (VRC(k), ADR(k)) and (VRC(k+1), ADR(k+1)) are two data points and ADR(k)<ADR$_o$<ADR(k+1).

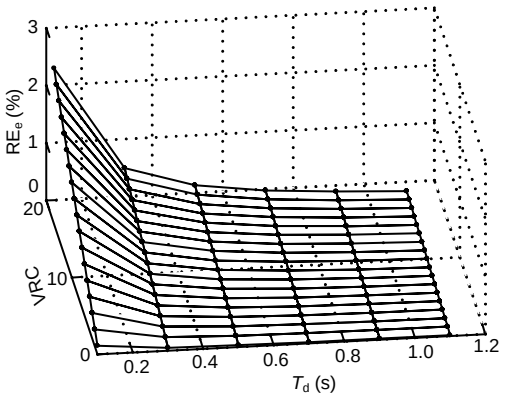

Fig. 3 Curves of RE_e while VRC intervals of 0.01 were used over a range from 0.01 to 20

2.4 Extended to arterial blood pressure

Since it is based on the two-element Windkessel model and focuses on the shape of pulse during diastole, we conjecture that the NSM can be applied to ABP. Also, as the error of the NSM mainly results from the interpolation, the same step size is competent for ABP. To test those hypotheses, we established a simulation model of the cardiovascular system with qin(t) as the input:

$$\mathrm{qin}(t)=\begin{cases}q_0\sin\dfrac{\pi t}{T-T_d}, & 0\le t\le T-T_d,\\ 0, & T-T_d\le t\le T,\end{cases} \tag{6}$$

where qin(t) is the instantaneous blood flow pumped into the arterial system, and T is the heart period. Then, we applied the NSM to estimate RC of output pressure pulse (PRC) from the simulation model.

The ability of the NSM to estimate PRC was judged on the relative error (RE_p) between the estimation (PRC_e) and actual (PRC_a) values:

$$\mathrm{RE}_p=\frac{\left|\mathrm{PRC}_e-\mathrm{PRC}_a\right|}{\mathrm{PRC}_a}\times 100\%. \tag{7}$$

3 Results

3.1 Experimental cases

Reliability of the NSM to estimate VRC is generally difficult to assess due to the absence of a gold standard for determining real values. Thus, we proposed to compare the behavior of the NSM with that of a reference method LSM. To reduce the probability of the convergent problem emerging in the NSM, we recommended selecting about 200 stable beats for each participant, as proposed by Lopez-Beltran (1998). VRC estimations from each of these beats of each individual with the LSM (VRC_{ls}) and NSM (VRC_{ns}) are summarized in Table 1. Individual variability made VRC distribute in diverse ranges. VRC_{ns} had a typical linear correlation with VRC_{ls} for each participant (r>0.927) and significantly different results were observed (P<0.01; paired t-test).

Linear regression equations were developed between VRC_{ls} and VRC_{ns} for each participant. Both slope and intercept had inter-personal variabilities. Figs. 4 and 5 show, as representative examples, the estimated values, as well as the linear regression curves of VRC_{ls} and VRC_{ns} obtained from participant one in the healthy group and participant nine in the general anesthesia group. Linear regression yielded VRC_{ns}=1.3154VRC_{ls}−0.2416; R^2=0.9831 and VRC_{ns} =1.2601VRC_{ls}−0.5107; R^2=0.9247, respectively.

Apparently, two model predicted curves during diastole for each beat can be obtained with VRC_{ls} and VRC_{ns}. To compare the performance of the two methods, we analyzed the fitness (R^2) of the

Table 1 VRC estimations with two methods for the twenty-one participants

Healthy group						
N	VRC_{ls}		VRC_{ns}		r	P
	Averge±SD	Range	Averge±SD	Range		
1	0.2259±0.0525	0.1238−0.4360	0.4004±0.0894	0.2209−0.7197	0.9989	**
2	0.5286±0.2017	0.2319−1.4310	0.4919±0.1452	0.2698−1.0344	0.9790	**
3	0.7855±0.3238	0.2679−2.1408	0.7230±0.2578	0.2796−1.5726	0.9839	**
4	0.2984±0.0952	0.1033−0.8159	0.5246±0.2097	0.1411−1.6598	0.9903	**
General anesthesia group						
N	VRC_{ls}		VRC_{ns}		r	P
	Averge±SD	Range	Averge±SD	Range		
1	0.4503±0.0969	0.3192−0.7361	0.5189±0.1198	0.3438−0.9428	0.9979	**
2	0.8872±0.5536	0.2352−5.2739	0.9649±0.60422	0.3859−5.3771	0.9875	**
3	0.3848±0.1618	0.1469−0.8624	0.5468±0.2004	0.2495−1.2209	0.9920	**
4	0.2996±0.0623	0.1903−0.5940	0.4031±0.0830	0.2660−0.7577	0.9957	**
5	1.2491±0.2253	0.8961−1.9654	1.3824±0.6479	0.7258−4.0878	0.9532	**
6	0.2235±0.0196	0.1639−0.2736	0.2742±0.0198	0.2169−0.3528	0.9992	**
7	0.2625±0.0325	0.1808−0.3261	0.3341±0.0470	0.2437−0.4632	0.9953	**
8	0.2939±0.0562	0.1641−0.5361	0.4269±0.0732	0.2385−0.7706	0.9981	**
9	0.8917±0.4729	0.5099−4.5390	1.1388±0.8194	0.5482−7.0317	0.9803	**
10	0.2711±0.0580	0.1160−0.5766	0.4200±0.0858	0.1815−0.8966	0.9941	**
11	0.7256±0.1237	0.4977−1.1438	0.8355±0.1795	0.5245−1.4682	0.9979	**
12	0.2482±0.0601	0.1735−0.4558	0.3220±0.0830	0.2145−0.6043	0.9981	**
13	0.7905±0.3138	0.1984−2.1537	1.0304±0.5012	0.2943−2.6975	0.9750	**
14	1.0367±0.2579	0.3889−1.9500	2.1250±1.0012	0.4872−5.1846	0.9269	**
15	0.4850±0.0497	0.3722−0.6710	0.5363±0.0564	0.4257−0.7188	0.9996	**
16	0.2236±0.0359	0.1559−0.3702	0.3359±0.0478	0.2459−0.5272	0.9993	**
17	0.5182±0.1589	0.2585−1.0833	0.5791±0.1422	0.3380−0.9509	0.9961	**

** represents P<0.01 in the t-test; VRC_{ls} and VRC_{ns}: VRC estimated by the LSM and NSM; r: correlation coefficient between VRC_{ls} and VRC_{ns}; N: sample number of each participant in the healthy and the general anesthesia groups, respectively

generated approximate curves, and the total running time of 200 beats for each participant. In the LSM, R^2 ranged from 0.92 to 0.99 and averaged as 0.985, with the running time varying from 0.0191 to 0.0233 s. Yet, in the NSM, the foregoing were 0.90 to 0.99, 0.979 in average, and 0.0002 to 0.0003 s, respectively. Original diastolic PPG with two approximate curves of four representative beats are shown in Fig. 6. Compared with VRC_{ns}, we found VRC_{ls} might exceed the reasonable range because the LSM just focused on high goodness of fit while the NSM limited the interpolation in the normal physiological range (Fig. 6a). Figs. 6b−6d indicated that the fitnesses were close, but decreased with increment of the difference between the original pulse and approximate curves and the two estimates were

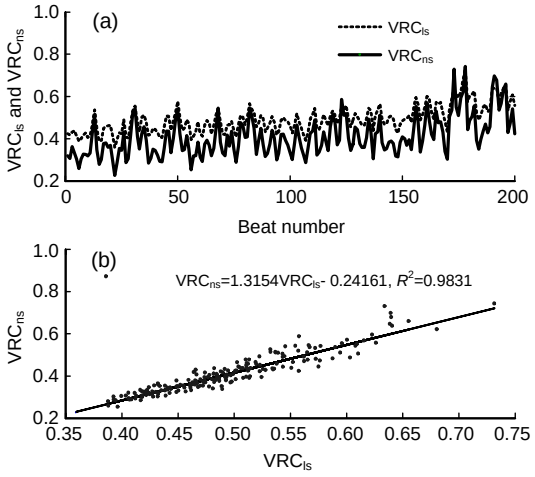

Fig. 4 (a) Values of VRC_{ls} and VRC_{ns} obtained from participant one in the health group; (b) Relationship between VRC_{ns} and VRC_{ls}

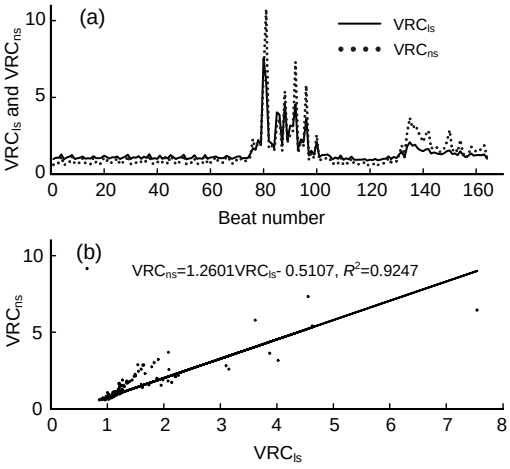

Fig. 5 (a) Values of VRC_{ls} and VRC_{ns} obtained from participant nine in the general anesthesia group; (b) Relationship between VRC_{ns} and VRC_{ls}

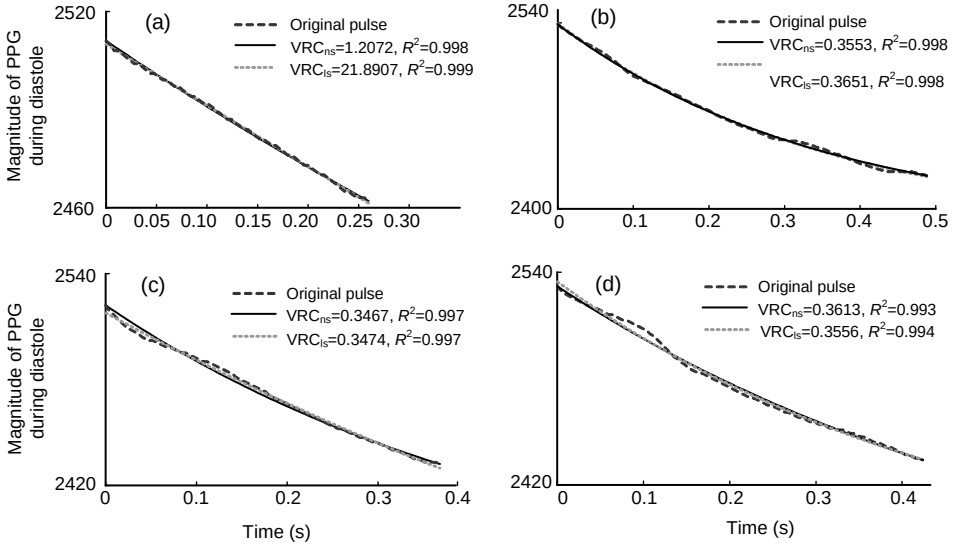

Fig. 6 Original diastolic PPG pulse with two approximate curves of four representative beats

(a) One typical beat whose VRC_{ls} other than VRC_{ns} exceeds the reasonable range; (b)–(d) Three distinct beats whose VRC estimations with two methods are basically equivalent, and the goodnesses of fit of the two approximated curves with VRC_{ls} and VRC_{ns} are very close, but decrease with increment of the difference between original pulse and approximate curves

Table 2 PRC estimations with the NSM and RE_p

PRC_a	$PRC_e(i)/RE_p(i)$						
	i=1, T_d=0.1 s	i=2, T_d=0.2 s	i=3, T_d=0.3 s	i=4, T_d=0.4 s	i=5, T_d=0.5 s	i=6, T_d=0.7 s	i=7, T_d=0.8 s
0.6	0.6001/0.02	0.5960/0.67	0.5984/0.27	0.6005/0.08	0.6003/0.05	0.6071/1.18	0.6041/0.68
1.2	1.2090/0.75	1.2002/0.02	1.2000/0.00	1.2240/2.00	1.2005/0.04	1.2191/1.59	1.2152/1.27
1.8	1.8162/0.90	1.8026/0.14	1.8010/0.06	1.8423/2.35	1.8007/0.04	1.8300/1.67	1.8249/1.38
2.4	2.4228/0.95	2.4046/0.19	2.4019/0.08	2.4584/2.43	2.4010/0.04	2.4405/1.69	2.4341/1.42
3.0	3.0291/0.97	3.0064/0.21	3.0027/0.09	3.0759/2.53	3.0012/0.04	3.0511/1.70	3.0431/1.44
3.6	3.6354/0.98	3.6081/0.23	3.6034/0.09	3.6922/2.56	3.6014/0.04	3.6615/1.71	3.6522/1.45
4.2	4.2415/0.99	4.2097/0.23	4.2042/0.10	4.3084/2.58	4.2017/0.04	4.2719/1.71	4.2611/1.45
4.8	4.8477/0.99	4.8113/0.24	4.8049/0.10	4.9244/2.59	4.8019/0.04	4.8824/1.72	4.8700/1.46

PRC_a: actual values of PRC setup in the simulation model; $PRC_e(i)$: values of PRC estimated with the NSM when T_d increases linearly from 0.1 to 0.7 s; $RE_p(i)$: values of the relative errors between PRC_a and $PRC_e(i)$ when T_d increases linearly from 0.1 to 0.7 s), %

basically the same. The results showed that the NSM was computationally efficient while maintaining a slightly lower fitting degree than the LSM.

3.2 Application to arterial blood pressure

Table 2 presented the values of PRC estimated with NSM and RE_p (Eq. (7)). In all these cases, PRC is well-estimated, with RE_p less than 3%. Therefore, we can confirm our hypothesis that the NSM is also suitable for ABP. Fig. 7 shows the response curves of RE_p intuitively.

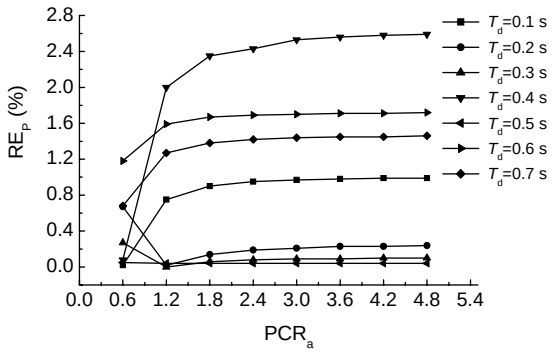

Fig. 7 Curves of RE_p responding to PRC_a and T_d

4 Discussion and conclusions

The decay time constant RC is a meaningful cardiovascular model parameter in clinical physiological monitoring and vascular assessment (Fogliardi *et al.*, 1996; Eyal *et al.*, 1997; Gnudi, 1998; Segers *et al.*, 1999; Bhattacharya *et al.*, 2001; Allen, 2007; Lu *et al.*, 2008). In summary, using or simply modifying the existing ABP shape methods could not achieve a satisfied estimation of RC from PPG, namely VRC. Therefore, we proposed a novel method, namely the NSM, to estimate VRC. The fundamental of the NSM was to establish a mathematic expression between a readily available parameter ADR and VRC. The intricacy of the expression compelled us to evaluate VRC using interpolation. Several alternative interpolation criteria, e.g., linear interpolation, polynomial interpolation, and adaptive Hermit spine interpolation (Li *et al.*, 2010b), are available for the estimation. Despite a lack of precision, we recommended utilizing the piecewise linear interpolation for the following reasons. First, it is computationally efficient, numerically stable, and easily realized in both PC and embedded systems. Second, owing to no gold standards for determining real overall compliance and resistance, VRC estimated in vitro is usually used for assessing changes in arterial properties. Thus, the demand for accuracy is not very high. Third, an appropriate step size of the linear interpolation not only simplifies the calculation, but guarantees the precision.

Comparing the estimates from measured PPG signals based on the two methods in vitro revealed a few discrepancies. VRC estimates with the NSM were generally close to, but not exactly equal to, the estimates with the LSM, which might be due to the following reasons.

1. Principal attention in the LSM was devoted to the high goodness of fit, while the major errors in the NSM resulted from the interpolation. An appropriate step size would improve accuracy. However, the fact that there are no international recognized standards in measurement technology and protocols for clinic PPG measurements (Allen, 2007), limits the reproducibility between different research centers. Thus, the

optimal step size in this paper might not be feasible for other researchers. An appropriate step size should be further determined according to Eq. (4) and the accuracy requirement. Certainly, the step size of 0.01 is sufficient without any obvious additional errors induced.

2. There was a constraint condition that both the onset and endpoint of diastole were on the model predicted curve to avoid the possibility of bad convergence or no convergence that would occur in the LSM.

The selection of onset and endpoint of diastole, in theory, makes no difference to the estimates of VRC because the diastolic pulse is fitted to a mon-exponential curve with the single decay time constant VRC according to the two-element Windkessel model. However, under real conditions, both perturbation and the phenomenon of pulse transmission (Fogliardi *et al.*, 1996; Eyal *et al.*, 1997; Alastruey *et al.*, 2009) are present. This often causes that the estimates of VRC depend on the selection of onset and endpoint of diastole. It is outside the scope of this paper to discuss which part is optimal, as many studies focus on the detection of fiducial points instead of the selection of diastolic part in the area of the PPG pulse. In this paper, we identified these fiducial points using differentials of different orders (Karamanoglu, 1997; Takazawa *et al.*, 1998; Li *et al.*, 2010a), and then chose the diastolic part, as proposed by Miyai *et al.* (2001).

A contribution of this paper is the establishment of a mathematic expression between a morphological parameter ADR and a cardiovascular model parameter VRC, and thus, to offer an alternative parameter for vascular assessment. ADR can be derived more easily from the PPG pulse than VRC. This is because ADR is readily acquired, while VRC may not be worked out, especially when the observed beat of pulse does not conform to the two-element Windkessel model. Hence, ADR can be regarded as an index for preliminary screening. For instance, if ADR is negative, we should give up estimating VRC. Therefore, we audaciously presume that ADR is a more useful alternative, which will play a similar role in cardiovascular status analysis. Further studies on this hypothesis will be examined in our future research.

References

Ahonen, J., Jokela, R., Uutela, K., Huiku, M., 2007. Surgical stress index reflects surgical stress in gynaecological laparoscopic day-case surgery. *British Journal of Anaesthesia*, **98**(4):456-461. [doi:10.1093/bja/aem035]

Alastruey, J., Parker, K.H., Peiro, J., Sherwin, S.J., 2009. Analysing the pattern of pulse waves in arterial networks: a time-domain study. *Journal of Engineering Mathematics*, **64**(4):331-351. [doi:10.1007/s10665-009-9275-1]

Allen, J., 2007. Photoplethysmography and its application in clinical physiological measurement. *Physiological Measurement*, **28**(3):R1-R39. [doi:10.1088/0967-3334/28/3/R01]

Bhattacharya, J., Kanjilal, P.P., Muralidhar, V., 2001. Analysis and characterization of photo-plethysmographic signal. *IEEE Transactions on Biomedical Engineering*, **48**(1):5-11. [doi:10.1109/10.900243]

Eyal, S., Oz, O., Eliash, S., Wasserman, G., Akselrod, S., 1997. The diastolic decay constant in spontaneously hypertensive rats versus WKY rats as an indicator for vasomotor control. *Journal of the Autonomic Nervous System*, **64**(1):24-32. [doi:10.1016/s0165-1838(97)00012-X]

Fogliardi, R., Burattini, R., Shroff, S.G., Campbell, K.B., 1996. Fit to diastolic arterial pressure by third-order lumped model yields unreliable estimates of arterial compliance. *Medical Engineering & Physics*, **18**(3):225-233. [doi:10.1016/1350-4533(95)00042-9]

Gnudi, G., 1998. New closed-form expressions for the estimation of arterial Windkessel compliance. *Computers in Biology and Medicine*, **28**(3):207-223. [doi:10.1016/S0010-4825(98)00008-0]

Haffty, B.G., O'Hare, N.E., Singh, J.B., Spodick, D.H., 1983. Noninvasive tracking of peripheral resistance by ear densitography. *Chest*, **83**(5):771-775. [doi:10.1378/chest.83.5.771]

Hashimoto, J., Chonan, K., Aoki, Y., Nishimura, T., Ohkubo, T., Hozawa, A., Suzuki, M., Matsubara, M., Michimata, M., Araki, T., *et al.*, 2002. Pulse wave velocity and the second derivative of the finger photoplethysmogram in treated hypertensive patients: their relationship and associating factors. *Journal of Hypertension*, **20**(12):2415-2422.

Huiku, M., Uutela, K., van Gils, M., Korhonen, I., Kymalainen, M., Merilainen, P., Paloheimo, M., Rantanen, M., Takala, P., Viertio-Oja, H., *et al.*, 2007. Assessment of surgical stress during general anaesthesia. *British Journal of Anaesthesia*, **98**(4):447-455. [doi:10.1093/bja/aem004]

Karamanoglu, M., 1997. A system for analysis of arterial blood pressure waveforms in humans. *Computers and Biomedical Research*, **30**(3):244-255. [doi:10.1006/cbmr.1997.1450]

Li, B.N., Dong, M.C., Vai, M.I., 2010a. On an automatic delineator for arterial blood pressure waveforms. *Biomedical Signal Processing and Control*, **5**(1):76-81. [doi:10.1016/j.bspc.2009.06.002]

Li, B.N., Dong, M.C., Vai, M.I., 2010b. Modelling cardiovascular physiological signals using adaptive

Hermite and wavelet basis functions. *IET Signal Processing*, **4**(5):588-597. [doi:10.1049/iet-spr.2009.0002]

Lopez-Beltran, E.A., Blackshear, P.L., Finkelstein, S.M., Cohn, J.N., 1998. Non-invasive studies of peripheral vascular compliance using a non-occluding photoplethysmographic method. *Medical and Biological Engineering and Computing*, **36**(6):748-753. [doi:10.1007/ BF02518879]

Lu, S., Zhao, H., Ju, K., Shin, K., Lee, M., Shelley, K., Chon, K.H., 2008. Can photoplethysmography variability serve as an alternative approach to obtain heart rate variability information? *Journal of Clinical Monitoring and Computing*, **22**(1):23-29. [doi:10.1007/s10877-007-9103-y]

Marcinkevics, Z., Kusnere, S., Aivars, J.I., Rubins, U., Zehtabi, A.H., 2009. The shape and dimensions of photoplethysmographic pulse waves: a measurement repeatability study. *Acta Universitatics Latviensis Biology*, **753**:99-106.

Millasseau, S.C., Guigui, F.G., Kelly, R.P., Prasad, K., Cockcroft, J.R., Ritter, J.M., Chowienczyk, P.J., 2000. Noninvasive assessment of the digital volume pulse: comparison with the peripheral pressure pulse. *Hypertension*, **36**(6):952-956.

Millasseau, S.C., Kelly, R.P., Ritter, J.M., Chowienczyk, P.J., 2003. The vascular impact of aging and vasoactive drugs: comparison of two digital volume pulse measurements. *American Journal of Hypertension*, **16**(6):467-472. [doi:10.1016/S0895-7061(03)00569-7]

Miyai, N., Miyashita, K., Arita, M., Morioka, I., Kamiya, K., Takeda, S., 2001. Noninvasive assessment of arterial distensibility in adolescents using the second derivative of photoplethysmogram waveform. *European Journal of Applied Physiology*, **86**(2):119-124. [doi:10.1007/s00421 0100520]

Randall, O.S., Vandenbos, G.C., Westerhof, N., Pot, F.O.M., 1984. Systemic compliance-does it play a role in the genesis of essential-hypertension. *Cardiovascular Research*, **18**(8):455-462. [doi:10.1093/cvr/18.8.455]

Reisner, A., Shaltis, P.A., McCombie, D., Asada, H.H., 2008. Utility of the photoplethysmogram in circulatory monitoring. *Anesthesiology*, **108**(5):950-958. [doi:10.1097/ALN.0b013e31816c89e1]

Segers, P., Verdonck, P., Deryck, Y., Brimioulle, S., Naeije, R., Carlier, S., Stergiopulos, N., 1999. Pulse pressure method and the area method for the estimation of total arterial compliance in dogs: sensitivity to wave reflection intensity. *Annals of Biomedical Engineering*, **27**(4):480-485. [doi:10.1114/1.192]

Seitsonen, E.R., Korhonen, I.K., van Gils, M.J., Huiku, M., Lotjonen, J.M., Korttila, K.T., Yli-Hankala, A.M., 2005. EEG spectral entropy, heart rate, photoplethysmography and motor responses to skin incision during sevoflurane anaesthesia. *Acta Anaesthesiologica Scandinavica*, **49**(3):284-292. [doi:10.1111/j.1399-6576.2005.00654.x]

Seki, K., 1988. Noninvasive measurement of elastic properties in human finger arteries: clinical data comparing blood pressure and funduscopic examination. *Heart and Vessels*, **4**(4):221-228. [doi:10.1007/BF02058590]

Shim, Y., Pasipoularides, A., Straley, C.A., Hampton, T.G., Soto, P.F., Owen, C.H., Davis, J.W., Glower, D.D., 1994. Arterial windkessel parameter estimation: a new time-domain method. *Annals of Biomedical Engineering*, **22**(1):66-77. [doi:10.1007/BF02368223]

Shimazu, H., Yamakoshi, K.I., Kamiya, A., 1986. Noninvasive Measurement of the volume elastic-modulus in finger arteries using photoelectric plethysmography. *IEEE Transactions on Biomedical Engineering*, **BME-33**(8):795-798. [doi:10.1109/TBME.1986.325906]

Stergiopulos, N., Segers, P., Westerhof, N., 1999. Use of pulse pressure method for estimating total arterial compliance in vivo. *American Journal of Physiology-Heart and Circulatory Physiology*, **276**(2):H424-H428.

Takazawa, K., Tanaka, N., Fujita, M., Matsuoka, O., Saiki, T., Aikawa, M., Tamura, S., Ibukiyama, C., 1998. Assessment of vasoactive agents and vascular aging by the second derivative of photoplethysmogram waveform. *Hypertension*, **32**(2):365-370.

Wang, J.J., O'Brien, A.B., Shrive, N.G., Parker, K.H., Tyberg, J.V., 2003. Time-domain representation of ventricular-arterial coupling as a windkessel and wave system. *American Journal of Physiology-Heart and Circulatory Physiology*, **284**(4):H1358-H1368.

Westerhof, N., Lankhaar, J.W., Westerhof, B.E., 2009. The arterial Windkessel. *Medical and Biological Engineering and Computing*, **47**(2):131-141. [doi:10.1007/s11517-008-0359-2]

Yamakoshi, K., Kamiya, A., 1987. Noninvasive measurement of arterial blood pressure and elastic properties using photoelectric plethysmography technique. *Medical Progress through Technology*, **12**(1-2):123-143.

Yin, F.C., Liu, Z.R., 1989. Estimating arterial resistance and compliance during transient conditions in humans. *American Journal of Physiology-Heart and Circulatory Physiology*, **257**(1):H190-H197.

Zahedi, E., Chellappan, K., Ali, M.A.M., Singh, H., 2007. Analysis of the effect of ageing on rising edge characteristics of the photoplethysmogram using a modified Windkessel model. *Cardiovascular Engineering*, **7**(4):172-181. [doi:10.1007/s10558-007-9037-5]